Advances in Engineering Software 47 (2012) 178–187

Contents lists available at SciVerse ScienceDirect

Advances in Engineering Software

journal homepage: www.elsevier.com/locate/advengsoft

Predicting torsional strength of RC beams by using Evolutionary Polynomial Regression

Alessandra Fiore [b,*], Luigi Berardi [b], Giuseppe Carlo Marano [a]

[a] Department of Environmental Engineering and Sustainable Development, Technical University of Bari, viale del Turismo 10, 74100 Taranto, Italy
[b] Department of Civil and Environmental Engineering, Technical University of Bari, via Orabona 4, 70125 Bari, Italy

ARTICLE INFO

Article history:
Received 19 April 2011
Received in revised form 19 July 2011
Accepted 2 November 2011
Available online 10 December 2011

Keywords:
Reinforced concrete beam
Evolutionary Polynomial Regression
Torsional strength
Building code
Theoretical model
Soft computing

ABSTRACT

A new view for the analytical formulation of torsional ultimate strength for reinforced concrete (RC) beams by experimental data is explored by using a new hybrid regression method termed Evolutionary Polynomial Regression (EPR). In the case of torsion in RC elements, the poor assumptions in physical models often result into poor agreement with experimental results. Nonetheless, existing models have simple and compact mathematical expressions since they are used by practitioners as building codes provisions.

EPR combines the best features of conventional numerical regression techniques with the effectiveness of genetic programming for constructing symbolic expressions of regression models. The EPR modeling paradigm allows to figure out existing patterns in recorded data in terms of compact mathematical expressions, according to the available physical knowledge on the phenomenon (if any). The procedure output is represented by different formulae to predict torsional strength of RC beam. The multi-objective search paradigm used by EPR allows developing a set of formulae showing different complexity of mathematical expressions as resulting into different agreement with experimental data.

The efficiency of such approach is tested using experimental data of 64 rectangular RC beams reported in technical literature. The input parameters affecting the torsional strength were selected as cross-sectional area of beams, cross-sectional area of one-leg of closed stirrup, spacing of stirrups, area of longitudinal reinforcement, yield strength of stirrup and longitudinal reinforcement, concrete compressive strength.

Those results are finally compared with previous studies and existing building codes for a complete comparison considering formulation complexity and experimental data fitting.

1. Introduction

In last decades a number of advancements has been observed in the field of reinforced concrete elements analysis; among them a number of remarkable research studies were aimed at overcoming problems in predicting final strength under different actions by using simple and effective formulations. Moreover differently from other situations, the torsional design of structural concrete elements is a complex problem which still remains an open question. In particular a more rational design formulation for RC structures under these specific actions still needs to be defined. The aim is to develop direct formulations which can be used without incurring the computational burden of numerical approaches like FEM. Such formulas, eventually, could be used for upgrading both existing best practices and current building codes. Moreover, such explicit formulations should be easily included into existing design codes, without significantly increasing the computational burden while improving prediction accuracy.

In this field (i.e. final torsional strength evaluation) there is an evident lack of efficient models to describe real physical behavior. In fact, for a given beam section, different current design codes might return quite different predictions which can vary by factors of more than two.

This is deeply different from other situations, such as the flexural strengths, whose predictions by the same codes may differ from each other by less than 10%. Actually, for flexure ultimate states some detailed models are used which take into account equilibrium, capability and non-linear stress–strain relationship of material. On the contrary, most of design equations for torsional strength derive directly from the equilibrium condition of the simple truss model theory proposed by Ritter and Morsch at the turn of the 20th century. This strong discrepancy is due to the difficulty in modeling the complex phenomena underlying the mechanical behavior of torsion by standard synthetic models.

* Corresponding author. Address: Politecnico di Bari, via Orabona 4, 70125 Bari, Italy. Tel.: +39 0805963525; fax: +39 0805963719.
E-mail address: a.fiore@poliba.it (A. Fiore).

0965-9978/$ - see front matter © 2011 Elsevier Ltd. All rights reserved.
doi:10.1016/j.advengsoft.2011.11.001

Nevertheless, several analytical and experimental studies have been reported in literature about torsional behavior of reinforced concrete (RC) members subjected to pure torsion or combination of torsion with other loadings, such as axial, shear and bending [1]. At present it is known that cross-sectional area of beam and its geometry, dimensions of closed stirrup, spacing of stirrups, cross-sectional area of one-leg of closed stirrup, yield strength of stirrup and longitudinal reinforcement and concrete compressive strength are the most important parameters involved. The effect of these variables on the torsional strength of RC beams has been extensively studied and several empirical approaches related to these variables have been investigated [2]. Test data are often used for validation, calibration or even development of above mentioned models.

However, although many experimental studies have been carried out to clarify the torsional behavior of RC beams, the estimation of the torsional strength of these structures still represents a complex task due to the high number of involved parameters [1].

In such a context, it is worthy to use some recently developed data analysis techniques aimed at discovering existing patterns in recorded data. A number of techniques has been proposed in recent years for identifying mathematical models of complex systems based on observed data [3]. Such techniques can be roughly ranked from white-box to black-box techniques depending on the level of prior information required/available. A white-box model is a system where all necessary information is available, i.e. the model is based on first principles (e.g. physical laws), variables are known and parameters have physical meaning. Conversely, black-box models do not require any prior information on the system in hand; they are data-driven or purely regressive models, for which neither functional form of relationships between variables nor numerical parameters are known and need to be estimated from training data. In between, there is a wide "palette" of gray-box models; they are conceptual models whose mathematical structure can be derived through conceptualization of physical phenomena or through simplification of known differential equations describing the phenomenon. These models usually need parameter estimation by means of input/output data analysis, although some information about underlying relationship is known.

White-box models, such as those developed for torsional ultimate strength prediction, have the advantage of describing the process being modeled using known mathematical relationships. However, the construction of white-box models can be difficult because the underlying mechanisms may not always be wholly understood, or because experimental results obtained in the laboratory environment do not correspond well to the prototype environment. Owing to these problems, approaches based on data-driven techniques are gaining considerable interest.

Among the existing data-driven techniques, Artificial Neural Networks (ANNs) and Genetic Programming (GP) are probably the most known. The first applications of Artificial Neural Network (ANN) date back to the early 1980s. Recently ANNs has been used as an effective tool to investigate different aspects of structural engineering, from analysis and design including constitutive laws of materials [4–6], to dynamics and structural damage [7,8]. A recent work [2] analyzed different ANNs for predicting the torsional strength of RC beams. The input parameters affecting the torsional strength were selected to be cross-sectional area of beams, dimensions of closed stirrups, spacing of stirrups, cross-sectional area of one-leg of closed stirrup, yield strength of stirrup and longitudinal reinforcement, steel ratio of stirrups, steel ratio of longitudinal reinforcement and concrete compressive strength. Each parameter was arranged in an input vector and a corresponding output vector included the torsional strength of RC beam.

However, in spite of their versatility as regression techniques, ANNs require the structure of a neural network to be identified *a priori* (e.g. model inputs, transfer functions, number of hidden layers, etc.). Furthermore, parameter estimation and over-fitting problems represent the principal disadvantages of model construction by ANN, as reported in [9]. These, in turn might result into lack of generalization capabilities of final models. Another difficulty with the use of ANNs is that they do not result into easily interpretable relationships which might help improve understanding of the physical phenomenon.

Genetic Programming (GP) is a modeling method that resorts to a population-based artificial intelligence technique to generate a structured representation of the system model. The model construction procedure mimics the natural evolutionary selection where the 'fittest' individuals (i.e. mathematical expressions of model) improve through successive generations. This technique allows a global exploration of the space of model expressions which can follow some user defined criteria.

On the one hand this strategy results into robust model search; on the other hand it potentially allows the user to gather additional information on system behavior by unveiling relationships between input and output data. Such features made the GP more appealing than ANNs for those context where the understanding of the system is still not completely known.

Among the GP methods, the so-called *symbolic regression* proposed by [10] is probably the most used. This technique uses the evolutionary search paradigm for developing explicit mathematical expressions of the model to fit a set of data points. However, the original GP method used to performing symbolic regression had some limitations since it does not perform a proper numerical estimation of model parameters (constants/coefficients) and it tends to produce expressions that grow in length during the evolutionary search [11]. Some notable attempts to mitigate those disadvantages have been reported for example by [12].

The Evolutionary Polynomial Regression (EPR) technique [13] has been introduced and continuously developed in the last years as an hybrid data-driven technique. EPR combines the effectiveness of evolutionary search for developing "transparent" and structured mathematical expression of input–output relationships with the advantage of classical numerical regression for parameter estimate. The EPR technique has been successfully applied to modeling a wide range of complex engineering problems including constitutive modeling of soils; stability of slopes; settlement of foundations; liquefaction of soils due to earthquake [14] and a number of other applications in Civil engineering [15–17]. A recent version of EPR, named EPR-MOGA, exploits Multi-Objective Genetic Algorithms (MOGAs) to search those model expressions which maximize accuracy of data and parsimony of mathematical expressions simultaneously. The main advantage of such approach is that EPR returns a set of explicit expressions with different accuracy to experimental data and different degree of complexity of mathematical structure of models. The analysis of such trade-off solutions between accuracy and complexity allows selecting those models which are better suited for specific applications.

This paper leverages such key features of EPR for developing explicit compact expressions to assess the ultimate torsional strength for RC beams.

To achieve these objectives, experimental data of 64 beams subjected to torsion are used. The just mentioned experimental data are obtained from [2], where the results of several tests performed by different authors such as Rasmussen and Baker [18], Koutchoukali and Belarbi [19], Fang and Shiau [20], and Hsu [21] are collected.

The experimental values of torsional strength are finally compared with both the relevant predictions of the main building codes, such as ACI-318-2005 [22], Eurocode-2 [23], TBC-500-2000 [24], CSA [25], BS8110 [26] and AS3600 [27], and the results obtained by EPR, in order to assess the efficacy of the proposed formulas.

2. Theories of torsional strength and torsion in the building standards

Theoretical models of torsional strength of reinforced concrete beams can be divided into two main theories: the skew-bending theory which was the base of the American Code up to 1995 and the space truss analogy which can be considered the base of the current American code and of the European model code.

The skew-bending theory was first proposed by Lessig in 1958 [28] and subsequently refined by Collins et al. [29] and Zia and Hsu [30]. This model is based on the assumption of a skew failure surface, which arises from an helical crack on three faces of a rectangular beam, while a compression zone develops on the fourth face. According to this theory the internal torsional resistance derives from three contributions: the axial forces of stirrups, the shear-compression force of concrete and the dowel forces of longitudinal bars. On this topic Hsu [21] furnished a big contribution; after assessing that concrete core did not provide any source to the ultimate torsional strength, he concluded that the concrete contribution was mainly due to the shear resistance of the diagonal struts.

The space truss analogy was first proposed by Rausch in 1929 [31]. In Rausch's concept, concrete is separated by cracks into a series of constant angle helical members, which are assumed to interact with the longitudinal steel bars and the stirrups to form a space truss. The circulatory shear stresses developing in the cross-section of the space truss, produce an internal torque capable of resisting the applied torsional moment. Since the core does not influence the torsional strength, the beam can be considered to be equivalent to an ideal tubular element. After the first idea proposed by Rausch, other authors have contributed for new updated versions of the model, including the spalling of concrete cover, the effects of variable angle cracks and confined concrete, the influence of the diagonal cracking on the compressive strength of the concrete struts, that is the softening effect [32–34].

According to the current torsion provision of ACI-318-2005 [22], the torsional strength T_n is given by:

$$T_n = \frac{2A_0 A_{st} f_{yv}}{s} \cot\theta \tag{1}$$

with:

$$\cot\theta = \sqrt{\frac{A_{sl} f_{yl} s}{A_{st} f_{yv} p_h}} \tag{2}$$

where A_0 is the cross area enclosed by the shear flow path that can be set equal to 0.85 A_{sh}, A_{sh} being the area enclosed by the center of stirrups; θ is the angle of compression diagonals; f_{yl} is the yield strength of longitudinal torsional reinforcement; f_{yv} is the yield strength of closed stirrups; A_{sl} is the total area of longitudinal torsional reinforcement; p_h is the perimeter of the centerline of the outmost closed transverse torsional reinforcement; s is the spacing of stirrups; A_{st} is the cross-sectional area of one-leg of closed stirrup. Fig. 1 reports a graphic representation of such variables. Eq. (1) is obtained by taking into account only the resistance sources provided by closed stirrups and longitudinal steel bars, while the concrete contribution is neglected.

In Australian Standard AS3600 [27] and Canadian Standard CSA [25] the torsional strength T_n of concrete beams is expressed by the same formula as ACI-318-2005 [22].

The British Standards BS8110 [26] provide the following expression to calculate the torsional strength of RC structures:

$$T_n = \frac{0.8 x_1 y_1 (0.87 f_{yv}) A_{sv}}{s} \tag{3}$$

where $x_1 y_1 = A_{sh}$ and $A_{sv} = 2A_{st}$.

As to the Turkish Building Code TBC-500-2000 [24], the torsional resistance is expressed as follows:

$$T_n = \frac{2A_e A_{sl} f_{yl}}{2(x_1 + y_1)} \tag{4}$$

where A_e is the area enclosed by the lines connecting the barycenter points of the corner longitudinal reinforcing bars.

Finally the European Standard Eurocode 2 [23] furnishes three expressions representing respectively the torsional resistances provided by concrete, shear reinforcement and longitudinal steel bars:

$$T_n = 1.2\left(1 - \frac{f_c}{250}\right) f_c A_k t_{ef} \sin\theta\cos\theta \tag{5}$$

$$T_n = \frac{2A_k A_{st} f_{yv}}{s} \cot\theta \tag{6}$$

$$T_n = \frac{2A_k A_{sl} f_{yl}}{\mu_k} \tan\theta \tag{7}$$

In the above equations, coherently with the concept of equivalent thin-walled section, A_k is the area enclosed by the center-lines of the connecting walls; t_{ef} is the effective wall thickness, which can be taken equal A/u, A and u being respectively the total area and outer circumference of the cross-section; μ_k is the perimeter of the area A_k; f_c is the compressive strength of concrete. The final torsional strength is defined as the smaller value between Eqs. (5)–(7).

3. Introduction to Evolutionary Polynomial Regression

EPR can be defined as a non-linear global stepwise regression, providing symbolic formulae of models. It is global since the search for optimal mathematical expressions of model is based on the exploration of the entire space of formulas by leveraging a flexible coding of mathematical structures. EPR generalizes the original stepwise regression of [35] by considering non-linear model structures (i.e., pseudo-polynomials) although they are linear with respect to regression parameters. Although the details about the main EPR paradigm are explained in the main reference works [13], a concise description is reported here for readers convenience.

One of the general model structures that EPR can manage is reported in the following equation:

$$\mathbf{Y} = a_0 + \sum_{j=1}^{m} a_j \cdot (\boldsymbol{X}_1)^{\mathbf{ES}(j,1)} \cdot \ldots \cdot (\boldsymbol{X}_k)^{\mathbf{ES}(j,k)} \cdot f\left((\boldsymbol{X}_1)^{\mathbf{ES}(j,k+1)} \cdot \ldots \cdot (\boldsymbol{X}_k)^{\mathbf{ES}(j,2k)}\right) \tag{8}$$

where m is the number of additive terms, a_j are numerical parameters to be estimated, $\boldsymbol{X}_i$ are candidate explanatory variables, $\mathbf{ES}(j,z)$ (with $z = 1,\ldots,2k$) is the exponent of the zth input within the jth term in Eq. (8), f is a function selected by the user among a set of possible alternatives (including no function selection). The exponents $\mathbf{ES}(j,z)$ are selected from a user-defined set of candidate values (which should include 0). In brief, the search for model structure is performed by exploring the combinatorial space of exponents to be assigned to each candidate input of Eq. (8). Thus, although exponent values could be any real number, they are coded as integers during the search procedure. It is worth noting that, when an exponent is = 0, relevant input $\boldsymbol{X}_i$ is basically deselected from the resulting equation. This, in turn, reduces the complexity of final mathematical expressions.

The search for model mathematical structures (i.e. combinations of exponents) is performed through a population based strategy that mimics the evolution of the individuals in nature. In particular it employs a Genetic Algorithm (GA) [36] whose individuals are represented by the sets of exponents in Eq. (8). It is worth noting that EPR mathematical structures, e.g. Eq. (8), are linear

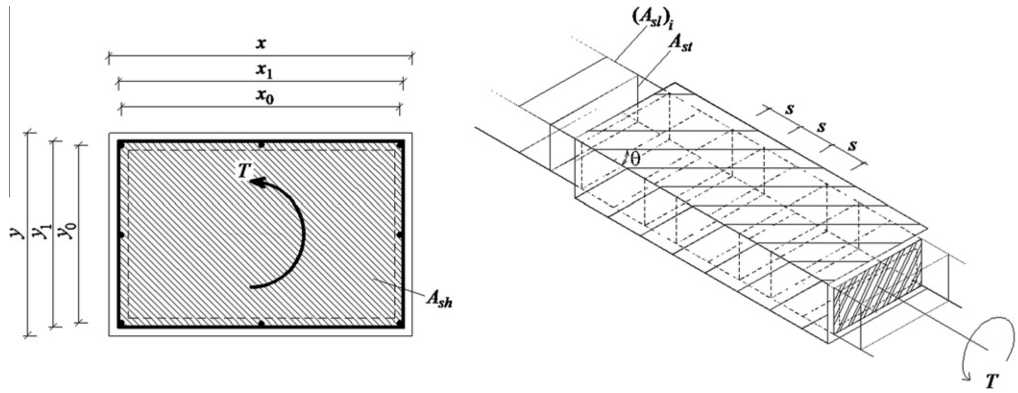

Fig. 1. Geometrical and mechanical characteristics affecting the torsional strength of a RC beam.

with respect to their parameters although not necessarily linear in their attributes (due to both exponents different from 1 and possible selection of function *f*). They are referred to as pseudo-polynomials since they are obtained by adding a number of monomial terms (i.e. argument of sum in Eq. (8)).

Model parameters are computed from data by solving a linear inverse problem in order to guarantee a two-ways (i.e., unique) relationship between each model structure and its parameters [13]. From a regressive standpoint, EPR may produce a non-linear mapping of data (like that achievable by Artificial Neural Networks although with few constants). These features, in turn, help avoiding over-fitting to training data thus improving generalization of resulting models. Furthermore, due to the search for model structure, EPR does not require a prior rigid selection of mathematical expressions and number of parameters.

3.1. Multi-objective EPR framework

Although the original EPR methodology proved to be effective, it used only one objective (i.e., the accuracy of data fitting) for exploring the space of solutions [13] while penalizing complex model structures using some penalization strategies. Nonetheless, the single-objective EPR methodology showed some shortcomings, such as (i) an exponentially decreasing performance in terms of computational time with the increasing of number of polynomial terms; (ii) the returned models are often difficult to interpret and inevitably prone to some subjective judgment for their selection (i.e., the selection process often biased by the analyst's experience rather than being purely based on mathematical/statistical criteria); (iii) while searching for models with m terms, it often happens that more parsimonious formulations (e.g., those having $m-1$ terms, that in this search run are degenerative case of the targeted models) are put away because there could be less parsimonious formulae that fit better the training data; and (iv) the introduction of unnecessary complexity (i.e., addition of new terms or combinations of inputs) that fits mostly random noise rather than the underlying phenomenon (i.e., a problem of over-fitting [37]).

The version of EPR used in [38], is known as EPR-MOGA and implements an evolutionary multi-objective genetic algorithm as optimization strategy based on the Pareto dominance criterion [39]. EPR-MOGA explores the space of m-term formulae using two or three among the following (conflicting) objectives: (i) the maximization of model accuracy, (ii) the minimization of the number of model coefficients (i.e. additive terms) and (iii) the minimization of the number of actually used model inputs (i.e. whose exponent is not 0 in the resulting model structure). The last two objectives represent as many measures of model parsimony, thus EPR-MOGA finally obtains a set of optimal solutions (i.e., the Pareto front) which can be considered as trade-offs between structural complexity and accuracy. The application of a multi-objective strategy leads to many advantages with respect to the original single objective approach: (i) improved computational efficiency; (ii) improved exploration of the space of solutions/formulae; (iii) automatic ranking of returned formulae according to structural complexity; (iv) enabled comparisons among formulae according to different criteria (e.g., selected inputs, structure, etc.); (v) trade-off between complexity and accuracy of the returned models; (vi) selection of different models suited for different modeling purposes [38].

The decision support framework for model selection allowed by EPR-MOGA can be summarized as follows (Fig. 2). After settings EPR-MOGA search options (candidate model attributes, candidate exponents for attributes, maximum number of parameters, etc.), like in classical EPR, and once a Pareto set of optimal models is obtained with respect to MOGA search objectives, the analyst is allowed to perform a further model selection. Such selection can be accomplished by considering: (i) the model structure with respect to physical insight related to the problem; (ii) similarities of mathematical structures among the Pareto set of models, as sorted according to model complexity; (iii) recurrent groups of variables in different models; and (iv) generalization performance of models as assessed in terms of both statistical indicators and mathematical parsimony.

Overall, the user is allowed to evaluate a set of models looking at different key aspects which encompass his/her knowledge of the physical phenomenon, reliability of experimental data used to build the model and/or final purpose of the model itself. This eventually results into a quite robust selection.

The EPR-MOGA employs a multi-objective genetic algorithm named OPTImized Multi-Objective Genetic Algorithm (OPTIMOGA), whose details are provided in [17]. It is worth noting that, due to the integer coding of decision variables adopted in EPR paradigm, the space of decision variables is discrete and combinatorial. In addition, the number of models on the Pareto front is usually not too large. Additionally, the Latin Hypercube sampling technique [40] is adopted for initializing the population of solutions although it was experimented that EPR-MOGA results are neither significantly influenced by initialization nor by MOGA search settings (e.g., reproduction, initialization, mutation rate, crossover rate, etc.).

The present analyses have been performed using the EPR MOGA-XL v.1 which is a Microsoft Office Excel add-in function freely available at www.hydroinformatics.it.

4. Prediction of the torsional strength of RC beams by EPR-MOGA

The experimental data considered have been obtained from [2], where the results of several tests performed by different authors

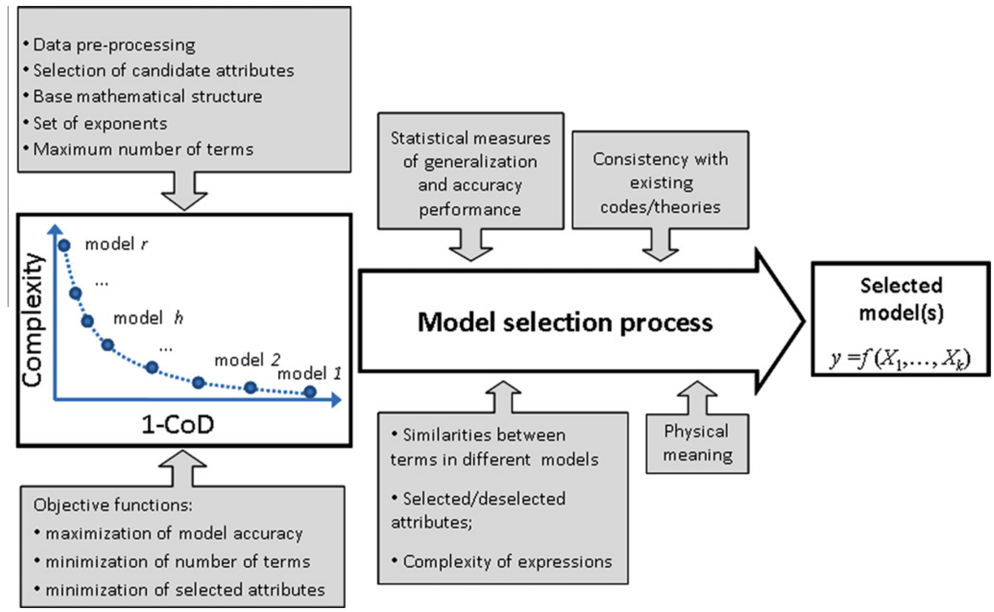

Fig. 2. Decision support framework for model selection based on MO-EPR strategy.

are summarized. These data report concrete strength ranging from normal to high, as well as the percentage of longitudinal reinforcement and stirrups. The test specimens refer to solid rectangular beams subjected to pure tension and do not include deep beams. The compressive strength of concrete ranges from 25.58 MPa to 109.8 MPa, the stirrup percentage ranges from 0.40% to 2.56%, the yielding stress of longitudinal reinforcement ranges from 314 MPa to 560 MPa, the yielding stress of stirrups ranges from 320 MPa to 672 MPa. In particular a total of 64 RC beams have been selected with different geometric parameters such as dimension of the cross-section (x,y), dimension of the closed stirrup (x_1,y_1), concrete compressive strength (f_c), spacing of stirrups (s), cross-sectional area of one-leg of closed stirrup (A_{st}), yield strength of closed stirrup (f_{yv}), total area of longitudinal torsional reinforcement (A_{sl}), yield strength of longitudinal torsional reinforcement (f_{yl}), steel ratio of stirrups (ρ_t) and steel ratio of longitudinal reinforcement (ρ_l). The remaining cases were discarded since they contained some apparent inconsistencies. The range of datasets is listed in Table 1.

The main objective of this study is to investigate the application of EPR-MOGA technique to get possible new formulations of torsional strength of RC beams able to reproduce the experimental data better than the existing code expressions [41]. In fact the correlation coefficients R^2 between experimental data and previsions of ACI-318-2005, AS3600, CSA (Eq. (1)), British Standards BS8110 (Eq. (3)), Turkish Building Code TBC-500-2000 (Eq. (4)) and Eurocode 2 (minimum value between Eqs. (5)–(7)) are respectively equal to 86.69%, 80.85%, 85.95% and 86.06%; thus there is some room for possible improvements.

4.1. EPR MOGA search settings

In order to make the proposed formulation useful for practical purpose, some compact expressions are sought for in terms of both number of parameters and explanatory variables involved. This, in turn, would facilitate their physical interpretation.

The base model structure reported in Eq. (8) is adopted with no function *f* selected; accordingly each additive monomial term is assumed to be a combination of the inputs raised to relevant exponents. Candidate exponents belong to the set [−2, −1.5, −1, −0.5, 0, 0.5, 1, 1.5, 2] in order to represent both linear and non-linear relationships as well as direct/inverse dependence between candidate input(s) and output (i.e. model target).

The maximum number *m* of additive terms in final expressions is assumed to be 2, which could be easily compared with the existing formulations. Candidate explanatory variables (i.e. model inputs) are A_{sh}, A_{st}, A_{sl}, s, p_h, f_{yv}, f_c; they have been selected by both looking at existing literature and performing some preliminary sensitivity analyses.

4.2. Selection of EPR MOGA models

Two EPR MOGA runs were finally performed, characterized by two different sets of exponents as detailed below and by the same set of input variables (A_{sh}, A_{st}/s, A_{sl}/p_h, f_{yv}, f_c). Models obtained from both EPR MOGA runs show different number of terms and explanatory variables as well as different accuracy. The model selection procedure takes into account some key aspects: agreement with experimental data, model parsimony and consistency with both physical insight about the torsional behavior of RC beams and previous building code formulations.

From among all models obtained, the following formulas have been selected (from this point on, the unit for T_n is [Nmm] and all the mechanical and geometrical quantities are expressed in N and mm respectively):

$$T_n = 0.34 \cdot A_{sh}^{1.5}\sqrt{\frac{A_{st}}{s}f_c}\ (R^2 = 94.48\%) \tag{9}$$

$$T_n = 2001.34 \cdot A_{sh} \cdot \frac{A_{st}}{s} \cdot f_{yv} \cdot \sqrt{\frac{A_{sl}}{p_h}\,\frac{s}{A_{st}}\,\frac{f_c}{(f_{yv})^3}}\ (R^2 = 94.78\%) \tag{10}$$

$$T_n = 0.036215 \cdot A_{sh}^{1.5}\sqrt{f_{yv}} + 73.445 \cdot A_{sh} \cdot \sqrt{\frac{A_{st}}{s}f_c\frac{A_{sl}}{p_h}}\ (R^2 = 97.75\%) \tag{11}$$

$$T_n = 0.68A_{sh} \cdot f_{yv} \cdot \sqrt{\frac{A_{sl}}{p_h}} + 1326.93 \cdot A_{sh} \cdot \frac{A_{st}}{s} \cdot f_{yv} \cdot \sqrt{\frac{A_{sl}}{p_h}\,\frac{s}{A_{st}}\,\frac{f_c}{(f_{yv})^3}}\ (R^2 = 97.41\%) \tag{12}$$

Table 1
Experimental data.

No	x (mm)	y (mm)	x_1 (mm)	y_1 (mm)	f_c (MPa)	s (mm)	A_{st} (mm^2)	f_{yv} (MPa)	A_{sl} (mm^2)	f_{yl} (MPa)	ρ_t (%)	ρ_l (%)	T_n (kN m)
FS-1	350	500	300	450	78.5	100	71.33	440	1196.6	440	0.61	0.68	92
F2-2	350	500	300	450	78.5	100	71.33	440	2027.2	410	0.61	1.16	115.1
FS-3	350	500	300	450	78.5	50	71.33	440	2027.2	410	1.22	1.16	155.3
FS-4	350	500	300	450	78.5	50	71.33	440	2865	520	1.22	1.64	196
FS-5	350	500	300	450	78.5	55	126.7	440	3438	560	1.97	1.96	239
FS-6	350	500	300	450	68.4	90	71.33	420	1719	500	0.68	0.98	126.7
FS-7	350	500	300	450	68.4	80	126.7	360	1719	500	1.36	0.98	135.2
FS-8	350	500	300	450	68.4	90	71.33	440	2865	500	0.68	1.64	144.5
FS-9	350	500	300	450	35.5	100	71.33	440	1191.6	440	0.61	0.68	79.7
FS-10	350	500	300	450	35.5	100	71.3	44	2027.2	410	0.61	1.16	95.2
FS-11	350	500	300	450	35.5	50	71.33	440	2027.2	410	1.22	1.16	116.8
FS-12	350	500	300	450	35.5	50	71.33	440	2865	520	1.22	1.64	138
FS-13	350	500	300	450	35.5	55	126.7	440	3438	560	1.97	1.96	158
FS-14	350	500	300	450	35.5	90	71.33	420	1719	500	0.68	0.98	111.7
FS-15	350	500	300	450	35.5	80	126.7	360	1719	500	1.36	0.98	125
FS-16	350	500	300	450	35.5	90	71.33	420	2865	500	0.68	1.64	117.3
KB-1	203	305	165	267	39.6	108	71.33	373	506.8	386	0.92	0.82	19.4
KB-2	203	305	165	267	64.6	108	71.33	399	506.8	386	0.92	0.82	18.9
KB-3	203	305	165	267	75	108	71.33	373	506.8	386	0.92	0.82	21.1
KB-4	203	305	165	267	80.6	108	71.33	399	506.8	386	0.92	0.82	19.4
KB-5	203	305	165	267	93.9	108	71.33	386	506.8	386	0.92	0.82	21
KB-6	203	305	165	267	76.2	102	71.33	386	506.8	386	0.98	0.82	18.4
KB-7	203	305	165	267	72.9	95	71.33	386	649.46	373	1.05	1.05	22.5
KB-8	203	305	165	267	75.9	90	71.33	386	760.2	373	1.11	1.23	23.7
KB-9	203	305	165	267	76.7	70	71.33	386	794.4	380	1.42	1.28	24
HS-1	254	381	215.9	342.9	27.58	152.4	71.33	341.29	508	313.71	0.54	0.52	22.3
HS-2	254	381	215.9	342.9	28.61	181.1	126.7	319.92	635	316.47	0.81	0.66	29.3
HS-3	254	381	215.9	342.9	28.06	127	126.7	319.92	762	327.5	1.15	0.79	37.5
HS-4	254	381	215.9	342.9	30.54	92.2	126.7	323.56	889	319.92	1.59	0.92	47.3
HS-5	254	381	215.9	342.9	29.03	69.9	126.7	321.3	1016	332.33	2.09	1.05	56.2
HS-6	254	381	215.9	342.9	28.82	57.2	126.7	322.67	1143	331.64	2.56	1.18	61.7
HS-7	254	381	215.9	342.9	25.99	127	126.7	318.54	508	319.92	1.15	0.52	26.9
HS-8	254	381	215.9	342.9	26.75	57.2	126.7	319.92	508	321.99	2.56	0.52	32.5
HS-9	254	381	215.9	342.9	28.82	152.4	126.7	342.67	762	319.23	0.96	0.79	29.8
HS-10	254	381	215.9	342.9	26.48	152.4	126.7	341.98	1143	334.4	0.96	1.18	34.4
HS-11	254	381	215.9	342.9	26.61	152.4	71.33	337.84	508	333.02	0.54	0.52	22.4
HS-12	254	381	215.9	342.9	25.58	181.1	126.7	330.95	635	322.67	0.81	0.66	27.7
HS-13	254	381	215.9	342.9	28.41	127	126.7	333.02	762	341.67	1.15	0.79	40.2
HS-14	254	381	215.9	342.9	30.61	92.2	126.7	333.02	889	330.26	1.59	0.92	47.9
HS-15	254	381	215.9	342.9	29.85	149.4	71.33	353.01	635	326.12	0.55	0.66	30.4
HS-16	254	381	215.9	342.9	30.54	104.9	71.33	357.15	762	328.88	0.79	0.79	40.6
HS-17	254	381	215.9	342.9	26.75	139.7	126.7	326.12	889	321.99	1.05	0.92	43.8
HS-18	254	381	215.9	342.9	26.54	104.9	126.7	326.81	1016	318.54	1.39	1.05	49.6
HS-19	254	381	215.9	342.9	27.99	82.6	126.7	330.95	1143	335.09	1.77	1.18	55.7
HS-20	254	381	215.9	342.9	29.37	69.9	126.7	340.6	2288	317.85	2.09	2.36	60.1
HS-21	254	381	215.9	342.9	45.23	98.6	71.33	348.87	635	325.43	0.84	0.66	36
HS-22	254	381	215.9	342.9	44.75	127	126.7	333.71	762	343.36	1.15	0.79	45.6
HS-23	254	381	215.9	342.9	44.95	92.2	126.7	326.12	889	315.09	1.59	0.92	58.1
HS-24	254	381	215.9	342.9	45.02	69.9	126.7	325.43	1016	310.26	2.09	1.05	70.7
HS-25	254	381	215.9	342.9	45.78	57.2	126.7	328.88	1143	325.43	2.56	1.18	76.7
HS-26	254	508	215.9	469.9	29.79	187.5	71.33	339.22	508	321.99	0.4	0.39	26.8
HS-27	254	508	215.9	469.9	30.89	120.7	71.33	333.71	635	322.67	0.63	0.49	40.3
HS-28	254	508	215.9	469.9	26.82	155.7	126.7	327.5	762	338.53	0.87	0.59	49.6
HS-29	254	508	215.9	469.9	28.27	114.3	126.7	341.98	889	325.43	1.18	0.69	64.9
HS-30	254	508	215.9	469.9	26.89	85.9	126.7	327.5	1016	330.95	1.57	0.79	72
HS-31	254	508	215.9	469.9	29.92	127	126.7	349.56	1144	334.4	1.06	0.89	39.1
HS-32	254	508	215.9	469.9	30.96	146.1	126.7	322.67	1430	319.23	0.92	1.11	52.7
HS-33	254	508	215.9	469.9	28.34	104.9	126.7	328.88	1716	321.99	1.28	1.33	63.3
HS-34	254	508	215.9	215.9	27.03	215.9	71.33	341.29	381	341.29	0.22	0.3	11.3
HS-35	254	508	215.9	215.9	26.54	117.6	71.33	344.74	508	334.4	0.41	0.39	15.3
HS-36	254	508	215.9	215.9	26.89	139.7	126.7	329.57	635	330.95	0.61	0.49	20
HS-37	254	508	215.9	215.9	27.17	98.6	126.7	327.5	762	336.46	0.86	0.59	25.3
HS-38	254	508	215.9	215.9	27.23	73.2	126.7	328.88	889	328.19	1.16	0.69	29.7
HS-39	254	508	215.9	215.9	27.58	54.1	126.7	327.5	1016	315.78	1.57	0.79	34.2

Although the EPR MOGA search for models is based on Coefficient of Determination (COD) as defined in [13], model performances are reported in terms of R^2 in order to allow a straight comparison with code provisions and alternative methods discussed in [1,2].

Expressions (9) and (11) are obtained by considering the set of exponents [−2, −1.5, −1, −0.5, 0, 0.5, 1, 1.5, 2], but in this way the physical insight of the problem is not easily recognizable. On the contrary in expressions (10) and (12) exponents belonging to the set [−1, −0.5, 0, 0.5, 1] are assumed; this choice allows to obtain models similar to the building code formulations and therefore to preserve the physical insight on the problem. In particular, putting $f_{yv} = f_{ys}$, Eq. (10) differs from Eq. (1) only for the factor $1177.26\sqrt{f_c/(f_{yv})^3}$.

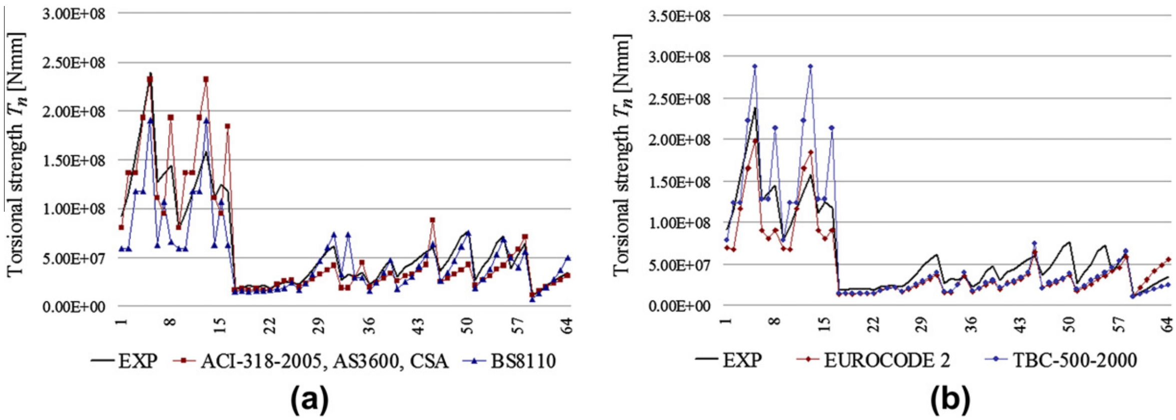

Fig. 3. Comparison between the experimental data (EXP) and the code data.

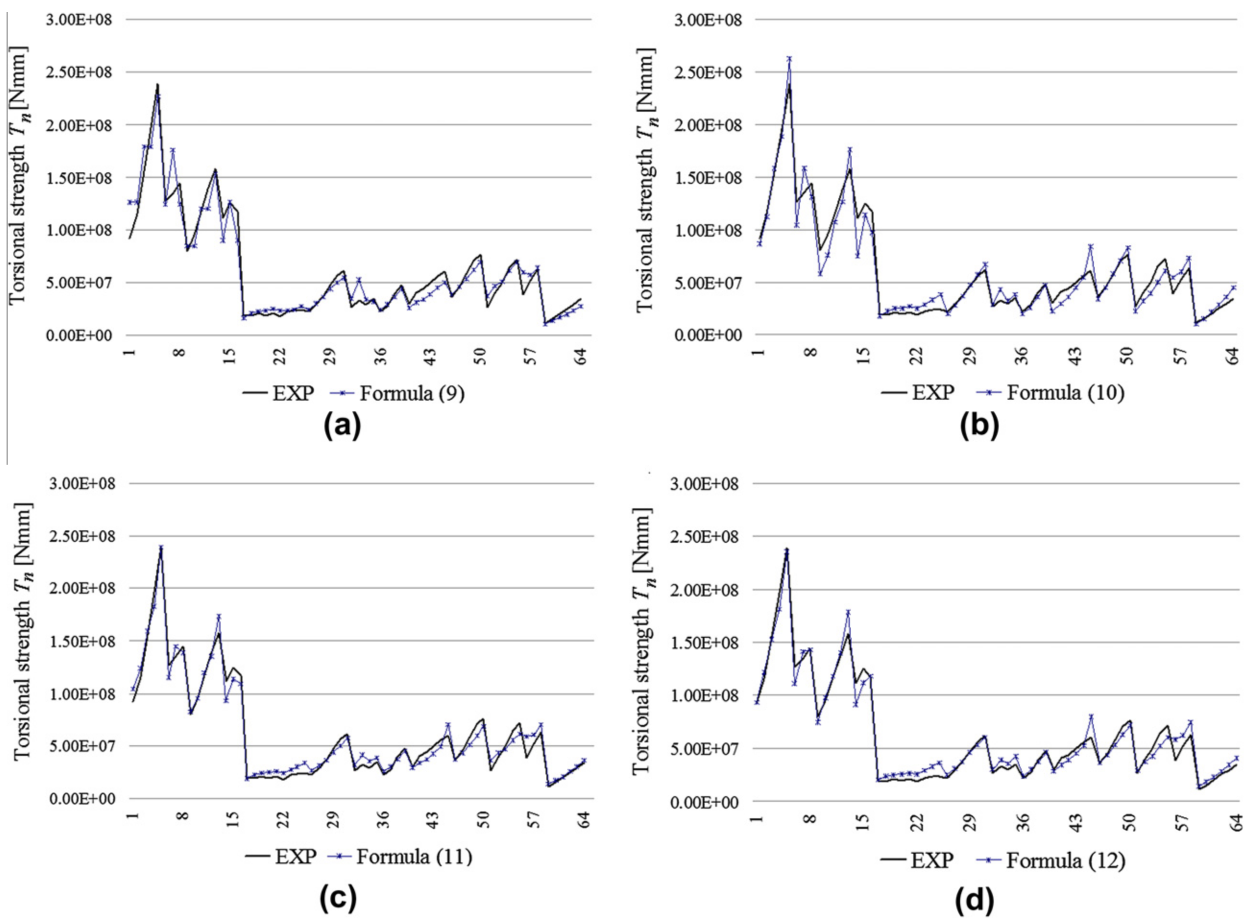

Fig. 4. Comparison between the experimental data (EXP) and the MO-EPR models (a-Eq. (9), b-Eq. (10), c-Eq. (11), d-Eq. (12)).

Fig. 3 shows a comparison between the experimental data and the code previsions (Eqs. (1), (3)–(7)); in Fig. 4a–d the experimental data are compared with the formulae (9)–(12), respectively. It is evident that all the proposed models are quite more accurate than the existing building code formulations although the complexity of their mathematical expressions are comparable. It is also worth noting that the increased accuracy is likely to descend from including the concrete strength f_c in calculating the torsional resistance. Vice versa, most of the existing building code approaches do not take this parameter into account when express the torsional strength by just one formula which includes the contributions of transversal and longitudinal reinforcements.

EPR MOGA models which consider the concrete strength show a significantly higher accuracy than building code formulation; nonetheless an accuracy up to $R^2 = 93.14\%$ can be obtained by neglecting f_c from candidate inputs and considering the same set of exponents as expressions (9) and (11):

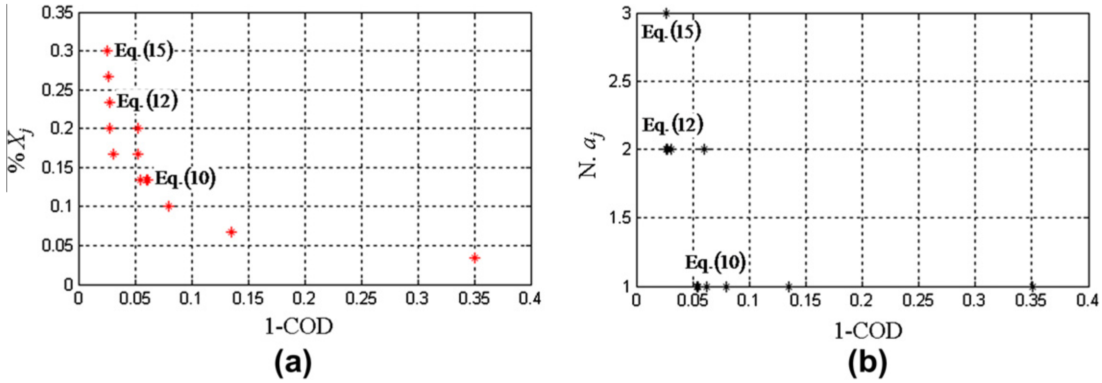

Fig. 5. Pareto fronts of expressions (10), (12), (15) in terms of (a) the percentage number of variables; and (b) the number of terms.

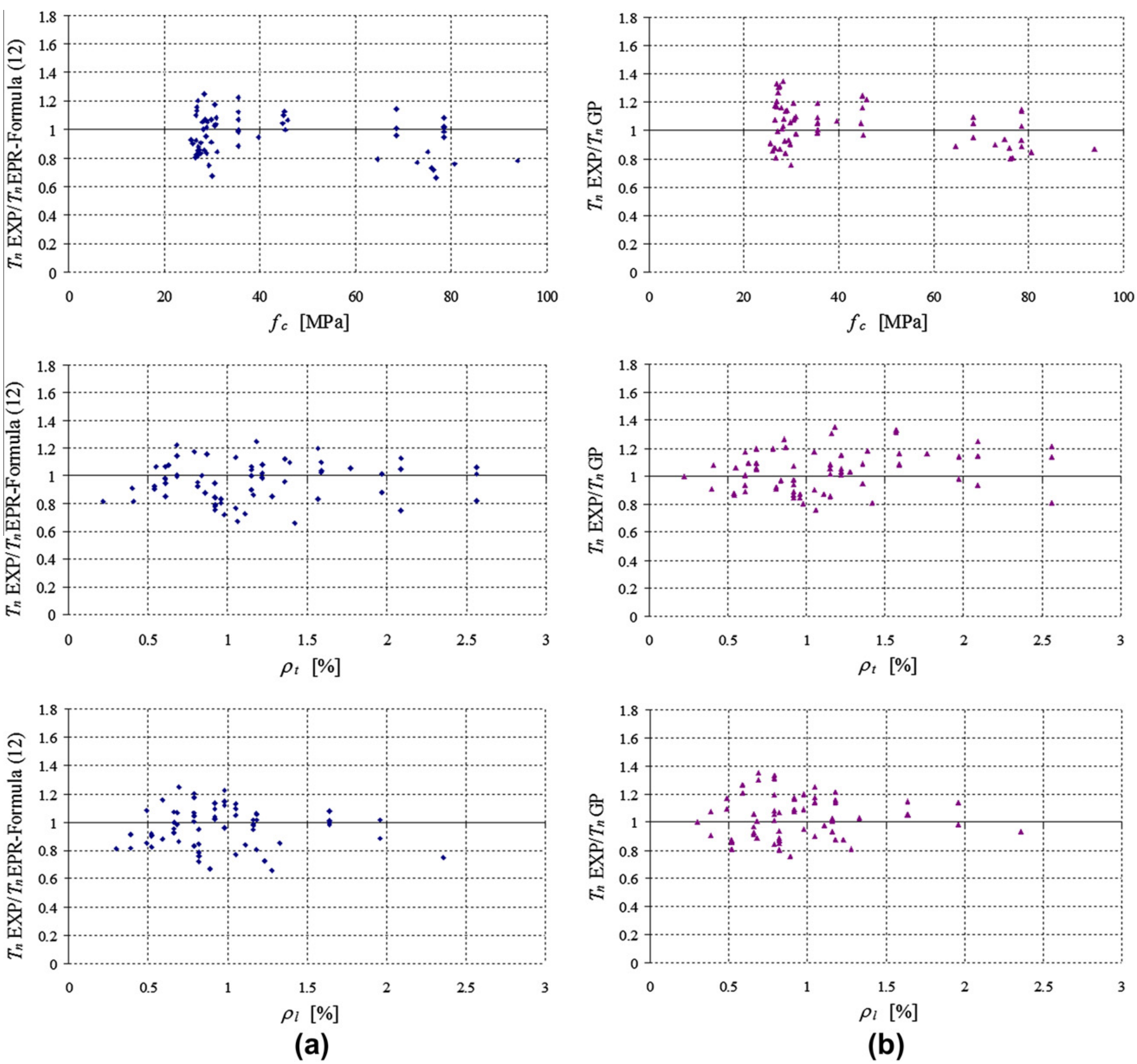

Fig. 6. Comparison between experimental and theoretical results in function of the main parameters: (a) formula (12), EPR; and (b) GP [1].

$$T_n = 0.95619 \cdot A_{sh} \cdot f_{yv}\sqrt{\frac{A_{sl}}{p_h}} + 0.52197 \cdot A_{sh} \cdot f_{yv}\sqrt{\frac{A_{st}}{s}\frac{A_{sl}}{p_h}} + 7.3408 \cdot A_{sh} \cdot \frac{A_{st}}{s} \cdot \sqrt{f_{yv}}\ (R^2 = 93.14\%) \quad (13)$$

In order to verify the effectiveness of EPR MOGA settings adopted, a further run was performed by allowing more additive terms in the final formulation. However, the slight increase of accuracy obtained does not justify the increase in model complexity. For example, the most accurate model with five terms, obtained by adopting the same settings of expressions (9) and (11), resulted into an accuracy equal to R^2 = 97.96%:

$$T_n = 42895193244.86 \cdot \left(\frac{A_{st}}{s}\right)^{1.5}\frac{\sqrt{f_c}}{f_{yv}^2} + 632206107.21 \times \sqrt{\frac{A_{sl}}{p_h}\frac{A_{st}}{s}A_{sh}}\frac{\sqrt{f_c}}{f_{yv}^2} + 0.0888\left(A_{sh}\frac{A_{sl}}{p_h}\right)^{1.5}\left(\frac{A_{st}}{s}\right)^{-1} + 0.0315A_{sh}^{1.5}\sqrt{f_{yv}} + 0.164A_{sh}^{1.5}\sqrt{\frac{A_{sl}}{p_h}\frac{A_{st}}{s}f_c} \quad (14)$$

Analogously, by adopting the same sets of exponents and input variables as expressions (10) and (12), the most accurate model is characterized by three terms and a R^2 = 97.49%:

$$T_n = 7.6525A_{sh}\sqrt{\frac{A_{sl}}{p_h}f_{yv}} + 0.27401A_{sh}f_{yv} + 69.2807A_{sh} \times \sqrt{\frac{A_{sl}}{p_h}\frac{A_{st}}{s}f_c}\ (R^2 = 97.49\%) \quad (15)$$

Fig. 5a and b shows the corresponding Pareto fronts, representing the accuracy (in terms of 1-COD), as returned by EPR MOGA XL tool, as a function respectively of the percentage number of variables (a) and of the number of additive terms (b). It emerges that expression (15) is significantly more complex than Eq. (12), even if the accuracy percentages of the two models are similar. This result confirms the efficacy of the selected formulations. Analogous conclusions can be derived by analyzing the Pareto fronts corresponding to expressions (9), (11), and (14), which are neglected here for sake of brevity.

Focusing on expression (12), the efficiency of EPR MOGA is further tested by comparing the corresponding performance with the predictions of ANN [2] and GP [1]. Fig. 6a shows the errors between the tests and EPR model in function of the variation of f_c, ρ_t and ρ_l. The same graphs referring to ANN and GP are reported in [2] and in Fig. 6b, respectively. From this comparison it emerges that the error between the tests and EPR is quite small with respect to ANN, while is similar to the GP case. Moreover while the values of torsional strength computed by using ANN are general lower than the experimental data, in the case of EPR and GP there is a balance between higher and lower values and this is preferable for structural safety. Nevertheless it is worth noting that, differently from GP, EPR formulation allows to preserve the physical insight of the problem; consequently the use of EPR is particularly suitable for practical purposes and for possible improvements of code provisions.

Finally by adopting Formula (10), graphs quite similar to Fig. 6a are obtained, with ratios between experimental data and EPR previsions ranging from 0.6 to 1.5. The above considerations are thus confirmed also in this case.

5. Conclusions

In the present paper new formulas for calculating the torsional strength of RC beams have been proposed. Differently from standard approaches, they are obtained by a new hybrid regression method termed Evolutionary Polynomial Regression (EPR). The efficiency of such approach has been tested by using experimental data of 64 rectangular RC beams reported in technical literature. The input parameters considered here have been selected by looking at existing code formulations to be directly comparable with these expressions. They are area enclosed by the center of stirrups, concrete compressive strength, spacing of stirrups, cross-sectional area of one-leg of closed stirrup, yield strength of reinforcement, total area of longitudinal torsional reinforcement, perimeter of centerline of outmost closed transverse reinforcement. Models obtained from EPR MOGA runs show different number of terms and explanatory variables as well as different accuracy. Among all the proposed models, the selected ones result more accurate than the existing building code formulations. Moreover they also represent the physical and mechanical insight on the problem. The increased accuracy probably descends from including the concrete strength in calculating the torsional one. Vice versa the codes in force neglect the concrete resistance when express the torsional strength by just one formula which includes the contributions of transversal and longitudinal reinforcements. Finally the authors advise that in prospective the use of this specific methodology (EPR) should be increased in defining code formulations for structural engineering, especially in those cases, like the present one, where poor mechanical models are available for physical description of phenomena.

References

[1] Cevik A, Arslan MH, Köroglu MA. Genetic-programming based modeling of RC beam torsional strength. KSCE J Civil Eng 2010;14(3):371–84.
[2] Arslan MH. Predicting of torsional strength of RC beams by using different artificial neural network algorithms and building codes. Adv Eng Softw 2010;41:946–55.
[3] Ljung L. System identification: theory for the user. 2nd ed. Upper Saddle River, New Jersey, USA: Prentice-Hall Inc.; 1999.
[4] Hadi MNS. Neural network applications in concrete structures. Comput Struct 2003;81(6):373–81.
[5] Inel M. Modeling ultimate deformation capacity of RC columns using artificial neural networks. Eng Struct 2007;29(3):329–35.
[6] Rafiq MY, Bugmann G, Easterbrook DJ. Neural network design for engineering applications. Comput Struct 2001;79(17):1541–52.
[7] Chen HM, Tsai KH, Qi GZ, Yang JCS, Amini F. Neural networks for structural control. J Comput Civil Eng 1995;9(2):168–76.
[8] Elcordy MF, Chang KC, Lee GC. Neural networks trained by analytically simulated damage states. J Comput Civil Eng 1993;7(2):130–45.
[9] Giustolisi O, Laucelli D. Increasing generalisation of input-output artificial neural networks in rainfall-runoff modelling. Hydrol Sci J 2005;50(3):439–57. doi:10.1623/hysj.50.3.439.65025.
[10] Koza JR. Genetic programming: on the programming of computers by natural selection. Cambridge: MIT Press; 1992.
[11] Davidson JW, Savic DA, Walters GA. Symbolic and numerical regression: experiments and applications. Inform Sci 2003;150:95–117. doi:10.1016/S0020-0255(02)00371-7.
[12] Soule T, Foster JA. Effects of code growth and parsimony pressure on populations in genetic programming. Evolution Comput 1999;6(4):293–309.
[13] Giustolisi O, Savic DA. A symbolic data-driven technique based on evolutionary polynomial regression. J Hydroinform 2006;8(3):207–22. doi:10.2166/hydro.2006.020.
[14] Javadi AA, Rezania M. Application of artificial intelligence and data mining techniques in soil modelling. J Geomech Eng 2009;1(1):53–74.
[15] Berardi L, Kapelan Z, Giustolisi O, Savic D. Development of pipe deterioration models for water distribution systems using EPR. J Hydroinform 2008;10(2):113–26. doi:10.2166/hydro.2008.012.
[16] Doglioni A, Mancarella D, Simeone V, Giustolisi O. Inferring groundwater system dynamics from hydrological time-series data. Hydrol Sci J 2010;55(4):593–608. doi:10.1080/0262666.1003747556.
[17] Laucelli D, Giustolisi O. Scour depth modelling by a multi-objective evolutionary paradigm. Environ Model Softw 2011;26:498–509. doi:10.1016/j.envsoft.2010.10.013.
[18] Rasmussen LJ, Baker G. Torsion in reinforced normal and high strength concrete beams. Part-I: an experimental test series. ACI Struct J 1995;92(1):56–62.
[19] Koutchoukali NE, Belarbi G. Torsion of high strength reinforced concrete beams and minimum reinforcement requirement. ACI Struct J 2001;98(4):462–9.
[20] Fang IK, Shiau JK. Torsional behavior of normal and high strength concrete beams. ACI Struct J 2004;101(3):304–13.

[21] Hsu TTC. Torsion of structural concrete – behavior of reinforced concrete rectangular members. Torsion of structural concrete SP18-10 1968. ACI, Farmington Hills; p. 261–306.
[22] ACI Committee 318-2005. Building code requirements for structural concrete (ACI 318-05) and commentary (318R-05). Farmington Hills, Mich.: American Concrete Institute; 2005.
[23] European Standard. Eurocode 2. Design of concrete structures, prEN, 1992-1-1, Draft for stage 49, Commission of the European communities, European Committee for Standardization; 2002.
[24] TBC-500-2000. Requirements for design and construction of reinforced concrete structures. Turkish standards TS-500. Ankara; 2000.
[25] Canadian standard association. Design of concrete structures: structure design. CSA Standard, A23-3-94. Rexdale (Ontario): Canadian Standard Association; 1994.
[26] BS8110. Structural use of concrete. Part 2. British Standards; 1985.
[27] AS3600. Concrete structures. Standards Association of Australia; 2001.
[28] Lessig NN. Determination of carrying capacity of reinforced concrete elements with rectangular cross – section subjected to flexure with torsion. Institute Betona i Zhelezobetona 1959;5:5–28.
[29] Collins CD, Walsh PF, Archer FE, Hall AS. Reinforced concrete beams subjected to combined torsion and shear. UNICIV Report, No. R-14, University of New South Wales; 1965.
[30] Zia P, Hsu TTC. Design for torsion and shear in prestressed concrete. PCI J 2004;49(3):34–42.
[31] Rausch E. Design of reinforced concrete in torsion. Berlin: Technische Hochschule; 1929 [in German].
[32] Hsu TTC, Mo YL. Softening of concrete in torsional members – theory and tests. ACI J 1985;82(3):290–303.
[33] Wafa FF, Shihata SA, Ashour SA, Akhtaruzzaman AA. Prestressed high-strength concrete beams under torsion. J Struct Eng 1999;96(6):1049–58.
[34] Ashour SA, Samman TA, Radain TA. Torsional behavior of reinforced high strength concrete deep beams. ACI Struct J 1999;96(6):1049–58.
[35] Draper NR, Smith H. Applied regression analysis. New York: John Wiley & Sons; 1998.
[36] Goldberg DE. Genetic algorithms in search, optimization and machine learning. Reading, Massachusetts: Addison-Wesley; 1989.
[37] Crout NMJ, Tarsitano D, Wood AT. Is my model too complex? Evaluating model formulation using model reduction. Environ Model Softw 2009;24(1):1–7.
[38] Giustolisi O, Savic DA. Advances in data-driven analyses and modelling using EPR-MOGA. J Hydroinform 2009;11(3):225–36. doi:10.2166/hydro.2009.01.
[39] Van Veldhuizen DA, Lamont GB. Multiobjective evolutionary algorithms analyzing the state-of-the-art. Evolution Comput 2000;8(2):125–44.
[40] McKay M, Conover W, Beckman R. A comparison of three methods for selecting values of input variables in the analysis of output from a computer code. Technometrics 1979;211:239–45.
[41] Fiore A, Berardi L, Avakian J, Marano GC. Evolutionary polynomial regression as alternative way to predict the torsional strength of RC beams. In: The second international conference on soft computing technology in civil, structural and environmental engineering. Chaina, Crete (Greece); 6–9 September 2011.